Inorganic Chemistry

Article

pubs.acs.org/IC

Effect of Alkali-Metal Ions on the Local Structure and Luminescence for Double Tungstate Compounds $AEu(WO_4)_2$ (A = Li, Na, K)

Jinping Huang,* Jun Xu, Hongshan Luo, Xibin Yu, and Yikang Li

Department of Chemistry, Shanghai Normal University, 100 Guilin Road, Shanghai 200234, China

Supporting Information

ABSTRACT: The effect of alkali-metal ions on the local structure and luminescence properties for alkali-metal europium double tungstate compounds $AEu(WO_4)_2$ (A = Li, Na, K) has been investigated by a dual-space structural technique, atomic pair distribution function (PDF) analysis, and the Rietveld method of powder X-ray diffraction. The compounds $AEu(WO_4)_2$ (A = Li, Na) crystallize in the isostructure with the tetragonal space group $I41/a$ (No. 88) and show the same luminescence properties in spite of the different doped alkali metals. However, $KEu(WO_4)_2$ crystallizes in monoclinic symmetry with the space group $C2/c$ (No. 15). Compared with the two other counterparts, $KEu(WO_4)_2$ exhibits a more effective charge-transfer excitation, a larger Stokes shift, and a broader 612 nm emission band. This phenomenon is ascribed to the lower crystal symmetry in $KEu(WO_4)_2$, which influences bond distances and the coordination number of Eu^{3+}. Two complementary methods, the Rietveld method and PDF analysis, reveal that both $LiEu(WO_4)_2$ and $NaEu(WO_4)_2$ afford the same local surroundings of Eu^{3+}. The local structure determined by the Rietveld and PDF methods well account for the observed luminescent properties.

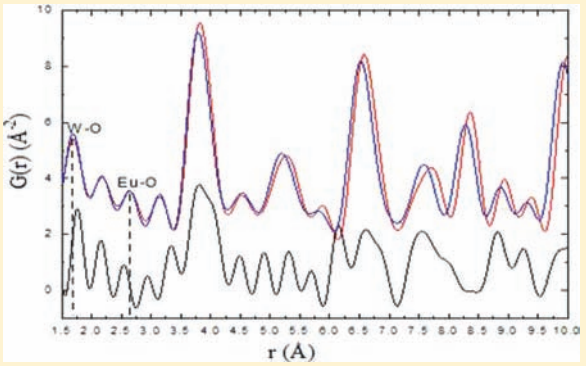

INTRODUCTION

White light-emitting diodes (W-LEDs) have emerged as the most promising solid-state lighting sources to replace conventional incandescent and fluorescent lamps because of their high reliability, long lifetime, low energy consumption, and environmentally friendly characteristics.[1] However, at present the search for red phosphors with high efficiency, excellent chemical stability, and effective absorption in the blue or UV region to improve the color-rendering index (Ra) of W-LEDs is still a challenging research task.[2,3] Eu^{3+}-activated tungstates and molybdates with scheelite-like ($CaWO_4$) structure have attracted much attention recently as interesting candidates for red-emitting phosphors. These materials have a broad and intense charge-transfer (CT) band in the UV region. The excitation intensity of Eu^{3+} in tungstates and molybdates at around 393 and 464 nm is prominently enhanced compared with that of Eu^{3+} in most hosts. For example, the composition $NaY_{0.5}Eu_{0.5}(WO_4)(MoO_4)$ shows a much higher light output than Y_2O_3S:Eu under 394 nm excitation.[4] This efficient long-wavelength-excited photoluminescence property of scheelite-type materials may find application in the production of red phosphors for LEDs. Remarkably, for alkali-metal-ion-containing luminescence materials, the effect of alkali-metal ions (Li, Na, and K) on the luminescence behavior of Eu^{3+}-activated tungstates and molybdates has been widely discussed.[5] It is found that the alkali-metal ions could not only enhance the luminescence intensity but also improve the color purity of the red phosphor. However, the effects of alkali-metal ions on the luminescence properties for various host matrixes are often inconsistent. For instance, Shi et al.[6] reported that under excitation of 395 and 465 nm, in the system of 0.24 concentration of Eu^{3+}-activated $CaWO_4$, the enhanced luminescence was regarded as the result of a charge compensator of alkali-metal ions. In addition, the luminescent intensity varied with Li^+, Na^+, and K^+ ions. With an increase of the alkali-metal ionic radius, the emission intensities gradually decreased. Therefore, the $Ca_{1-2x}Eu_xLi_xWO_4$ (x = 0.24) phosphor exhibits the strongest emission intensity. Li et al.[7] also found this discrepant influence on the system of $CaMoO_4$:Tb^{3+}, R^+ (Li^+, Na^+ and K^+), in which Na^+ ions have an optimal enhancement luminescence, however. It is proposed that the creation of oxygen vacancies due to the radius discrepancy of alkali-metal and Ca^{2+} ions is disadvantageous to the enhancement luminescence. Liu et al.[8] have investigated the dependence of the red emission intensity on the Eu^{3+} concentration (x) in a series of phosphors under excitation of 393 nm. They reported that for the phosphors $Ca_{1-2x}A_xMoO_4$:xEu^{3+} (A = K^+, Na^+, and Li^+), before 0.24 Eu^{3+}-doped concentrations, the emission intensity increases obviously with various alkali-metal ions. When the doped amount of Eu^{3+} ions is 0.24, K^+ ions have the best promotion effect. When the amount of dopant Eu^{3+} is increased again, red emission of Eu^{3+} is markedly enhanced by Na^+ and Li^+ ions.

Received: June 23, 2011
Published: October 26, 2011

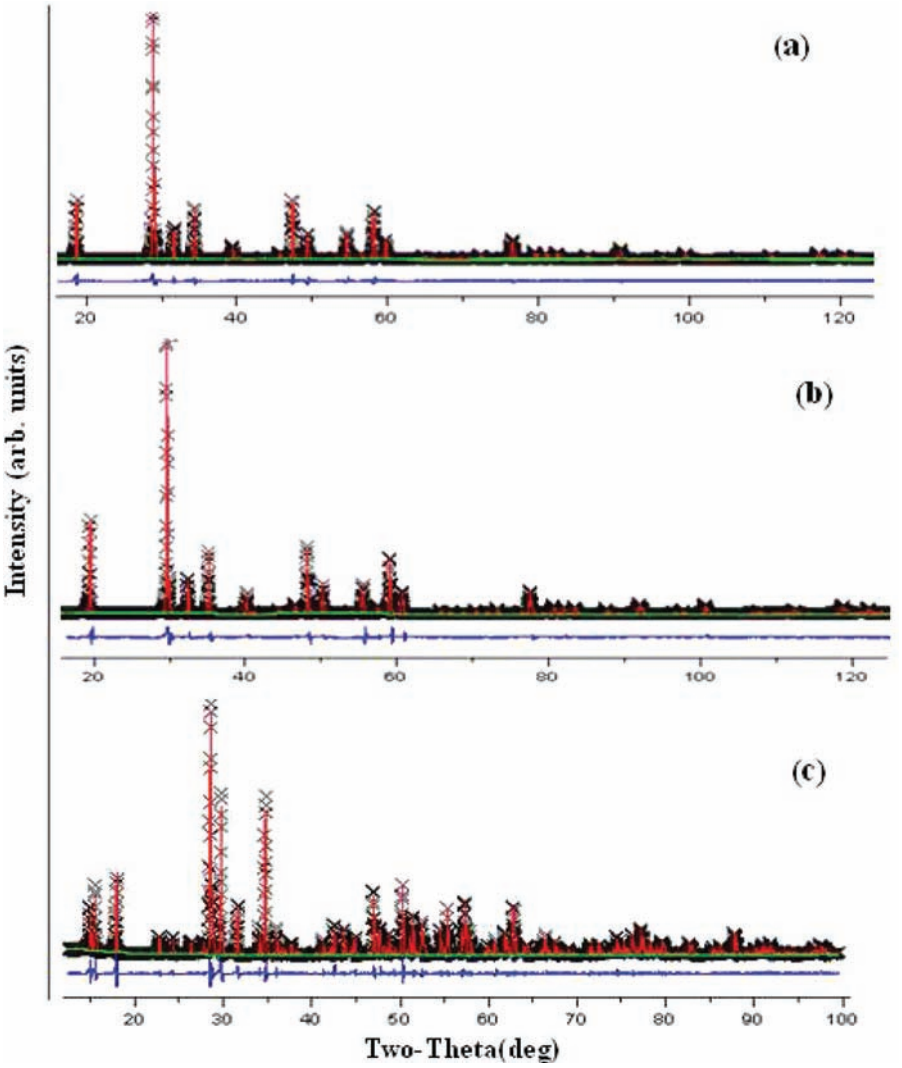

Figure 1. Rietveld refinement of X-ray diffraction patterns for (a) $LiEu(WO_4)_2$, (b) $NaEu(WO_4)_2$, and (c) $KEu(WO_4)_2$. The observed counts are indicated by thin crosses in black, and the calculated pattern is indicated by a solid line in red. The difference pattern below is in blue.

When the doped amount of Eu^{3+} is 0.5, Li^+ ions have the best effect. Actually, with the amount of Eu^{3+} up to 0.5, the phase $A_{0.5}Eu_{0.5}MoO_4$ (A = K^+, Na^+, and Li^+) formed, which is absolutely ascribed to another series of compounds. Recently, Guo et al.[9] reported that, in the double molybdate phosphors $AEu(MoO_4)_2$, the luminescence intensity of Eu^{3+} at the same temperature decreases in the order of $I_{Li} > I_{Na} > I_K$.

Taking into account the above discussion, to investigate the effect of alkali-metal ions on the emission intensity for alkali-metal-containing phosphors, we should keep the number of variables to a minimum. Specifically, the host structures and the doping concentration of alkali-metal ions and activator ions should be limited to those of comparable materials. Herein, we investigate the effect of alkali-metal ions on the local structure and luminescence properties for alkali-metal europium double tungstate compounds $AEu(WO_4)_2$ (A = Li, Na, K). This series of tungstates can be taken for the product of Eu^{3+} and an alkali-metal ion codoping scheelite-like ($CaWO_4$) structure with a maximum molar amount of Eu^{3+} and alkali of 0.5, wherein half the alkaline-earth ions are replaced by alkali metal and the other half by europium ions. For the family of $AEu(WO_4)_2$ (A = Li, Na, K), $LiEu(WO_4)_2$ and $NaEu(WO_4)_2$ adopt tetragonal space group $I41/a$ (No. 88), whereas $KEu(WO_4)_2$ crystallize in monoclinic symmetry with the space group $C2/c$ (No. 15). It is believed that alkali-metal ions not only modify the crystal structure but also distort the metal oxide polyhedron and disturb the sublattice structure around the luminescent center ions. By a dual-space structural technique combining the Rietveld and atomic pair distribution function (PDF) methods, it is possible to observe the effect of changes of the structure parameters on the luminescence brightness related to the site symmetry and the strength of the crystal field. The long-range ordering of a crystalline structure can always be accurately determined by analysis of the Bragg intensities and positions using the Rietveld method. However, local atomic displacements away from the crystallographic sites, if they exist, are reflected in the crystal structure only in terms of the large thermal or Debye–Waller factor, which cannot be easily separated from the lattice vibration. The PDF analysis technique takes all of the components of the diffraction data (Bragg peaks and diffuse scattering) into account and thus reveals both the longer range atomic order and the local deviations from it, yielding the atomic structure in terms of a small set of parameters such as a unit cell and atomic coordinates. In order to gain further insight into the structural features of alkali-metal europium double tungstate compound

dx.doi.org/10.1021/ic2013528 | *Inorg. Chem.* 2011, 50, 11487–11492

$AEu(WO_4)_2$ (A = Li, Na, K), both short- and long-range order in these compounds should be considered. We expect that PDF analysis could help in getting a more complete and accurate picture of the effect of alkali-metal ions on the local structure and luminescence properties for alkali-metal europium double tungstate compounds.

EXPERIMENTAL SECTION

Synthesis. The red phosphors $AEu(WO_4)_2$ (A = Li, Na, K) were prepared by the solid-state reaction. The starting materials $NaHCO_3$, Li_2CO_3, K_2WO_4, WO_3, and Eu_2O_3 were weighted according to the stoichiometric ratio.[10,11] After these powders were mixed thoroughly using a mortar, the homogeneous mixture was filled into a porcelain crucible and calcined in a muffle furnace for 10 h at a temperature of 750 °C. The products obtained were found to be polycrystalline and pink.

X-ray Diffraction Data Collection. X-ray diffraction patterns were collected on a Bragg–Brentano diffractometer (Rigaku D/Max-2000) with monochromatic Cu Kα radiation (λ = 1.5418 Å) of a graphite curve monochromator. The X-ray diffraction data for structure determination and refinement were collected from 2θ = 9 to 130°, with a step length of 0.02 (2θ) and counting times of 40 s/step. The Rietveld refinement software used is *GSAS*.[17]

PDF Data Acquisition. The experimental PDF, G exp(r), is the direct sine Fourier transformation of the normalized scattering intensity $S(Q)$. $S(Q)$ is obtained from the total scattering $I(Q)$ by experimental background subtraction, polarization correction, Compton scattering correction, and the atomic form factor of the material under investigation.[12] Here, sample and empty sample data were collected by a powder X-ray diffraction experiment from 2θ = 5 to 105°, with a step length of 0.01 (2θ) and counting times of 10 s/step, Q_{max} = 13.4 Å^{-1}. We used Mo Kα (λ = 0.717 07 Å; in-house Rigaku D/Max-2000) with a sealed X-ray tube source and a scintillation detector. The PDFs were generated using the program *PDFgetX2*.[13] *PDFgui*, a real-space nonlinear least-squares regression refinement program, was used to fit the structural model to all experimental PDFs.[14]

Optical Measurements. The excitation and emission spectra were measured at room temperature by a Varain Cary-Eclipse 500 spectrofluorometer with a 60 W xenon lamp as the excitation source.

RESULTS AND DISCUSSION

Phase Characterization and X-ray Structure Analysis.

The structures of the compositions were successfully refined by the *GSAS* suite.[17] The refined instrument and structure parameters were cell parameters, background, sample displacement, asymmetry by divergence,[18] spherical harmonics, etc. While $KEu(WO_4)_2$ has the lower symmetry $C2/c$ (No. 15), $NaEu(WO_4)_2$ (JCPDF 04-002-3849) and $LiEu(WO_4)_2$ (JCPDF 04-008-0354) crystallize in a scheelite structure with the space group of $I41/a$ (No. 88). Parts a–c of Figure 1 show the measured and calculated XRD patterns and the difference between them for $LiEu(WO_4)_2$, $NaEu(WO_4)_2$, and $KEu(WO_4)_2$, respectively. The crystal structure of $KEu(WO_4)_2$ presented here is different from that of the previous study.[15] The structure was refined using the atomic parameters from $KY(WO_4)_2$.[16] From Figure 1, it can be seen that all diffraction peaks match well and no traces of the additional peaks from other impurities were observed. The ionic radii of Li, Na, and K in eight coordination (CN8) are 1.06, 1.32, and 1.38 Å, respectively.[19–21] The smaller ionic radius of Li (CN8) directly results in the lattice contraction of $LiEu(WO_4)_2$. The formula unit volume of $KEu(WO_4)_2$ is 161.46, larger than those of both $LiEu(WO_4)_2$ (76.61) and $NaEu(WO_4)_2$ (78.87). This phenomenon is ascribed to the lower crystal symmetry of $KEu(WO_4)_2$. The crystallographic refinement data for these compounds are summarized in Table 1 (also see the Supporting Information, Tables S1–S3).

Table 1. Crystallographic Data of $LiEu(WO_4)_2$, $NaEu(WO_4)_2$, and $KEu(WO_4)_2$ at Room Temperature

	$LiEu(WO_4)_2$	$NaEu(WO_4)_2$	$KEu(WO_4)_2$
structure	tetragonal	tetragonal	monoclinic
space group	$I41/a$ (No. 88)	$I41/a$ (No. 88)	$C2/c$ (No. 15)
a (Å)	5.2115(3)	5.25997(3)	10.7043(2)
b (Å)	5.2115(3)	5.25997(3)	10.4730(2)
c (Å)	11.2823(4)	11.4030(1)	7.6082(2)
α (deg)	90.00	90.00	90.00
β (deg)	90.00	90.00	130.78(1)
γ (deg)	90.00	90.00	90.00
Z	4	4	4
volume of the unit cell (Å^3)	306.43(4)	315.49(1)	645.87(3)
R_p (%)	6.65	6.70	9.74
R_{wp} (%)	9.22	10.3	13.7
R_F (%)	4.23	3.56	4.34

In these structures, $LiEu(WO_4)_2$ and $NaEu(WO_4)_2$ are isostructures, which crystallize in the tetragonal space group $I41/a$ (No. 88). The Eu^{3+} ions are in the distorted EuO_8 octahedral coordination with S_4 symmetry. Compound $KEu(WO_4)_2$ crystallizes in monoclinic symmetry with the space group $C2/c$ (No. 15), in which Eu^{3+} ions are in the EuO_6 polyhedron with C_2 symmetry. The local surroundings of Eu^{3+} ions of these three compounds are presented in Figure 2. The

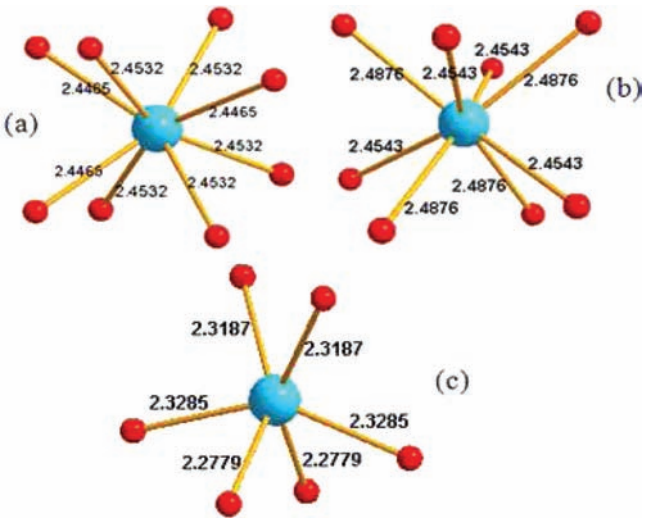

Figure 2. Surroundings of the luminescent center (Eu^{3+} in light blue and O^{2-} in red) of (a) $LiEu(WO_4)_2$, (b) $NaEu(WO_4)_2$, and (c) $KEu(WO_4)_2$.

selected bond distances and coordination numbers of $LiEu(WO_4)_2$, $NaEu(WO_4)_2$, and $KEu(WO_4)_2$ are listed in Table 2. The Eu–O bond distances in $LiEu(WO_4)_2$ and $NaEu(WO_4)_2$ are longer than that in $KEu(WO_4)_2$, while the Eu–O bond distance in $NaEu(WO_4)_2$ is longer than that in $LiEu(WO_4)_2$.

As mentioned above, the average structures have been determined by the Rietveld method. However, the local distortion information reflected in the crystal structure only in terms of the large thermal or Debye–Waller factor, which

dx.doi.org/10.1021/ic2013528 | Inorg. Chem. 2011, 50, 11487–11492

Table 2. Selected Bond Distances of $LiEu(WO_4)_2$, $NaEu(WO_4)_2$, and $KEu(WO_4)_2$

(a) Selected Bond Distances of $LiEu(WO_4)_2$		
bond type	CN	bond distance (Å)
LilEu–O1	4	2.4465(2)
LilEu–O2	4	2.4532(2)
W–O	4	1.7602(3)
(b) Selected Bond Distances of $NaEu(WO_4)_2$		
bond type	CN	bond distance (Å)
NalEu–O1	4	2.4543(2)
NalEu–O2	4	2.4876(2)
W–O	4	1.7866(1)

(c) Selected Bond Distances of $KEu(WO_4)_2$

bond type	CN	bond distance (Å)	bond type	CN	bond distance (Å)
W–O1	1	1.7974(2)	Eu–O1	2	2.2779(2)
W–O2	1	1.9963(2)	Eu–O2	2	2.3187(2)
W–O2	1	2.1046(1)	Eu–O3	2	2.3285(2)
W–O3	1	1.8343(3)	K–O1	2	2.9588(1)
W–O4	1	1.7814(3)	K–O4	2	2.7752(2)
W–O4	1	2.3576(3)	K–O4	2	2.8476(2)

can not be easily separated from the lattice vibration. The local surrounding information of the Eu^{3+} ions is expected to be obtained by PDF analysis. Fourier transform shows that what PDF physically represents is a real-space map of the atomic positions within a solid. It allows the direct analysis of real space, rather than reciprocal space, which is conceptually easier to visualize. From Figure 3, the W–O and Eu–O bond

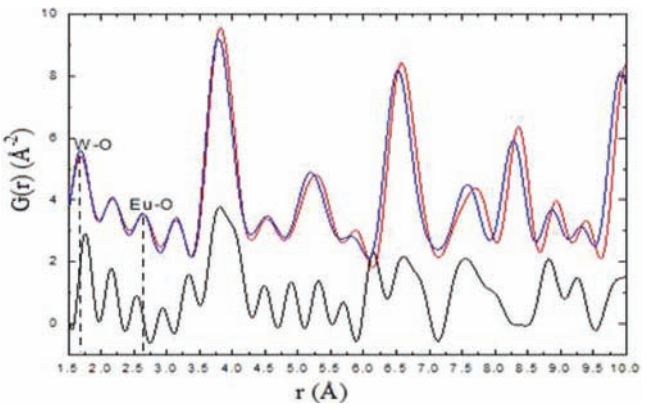

Figure 3. Experimental PDFs of $LiEu(WO_4)_2$ (blue), $NaEu(WO_4)_2$ (red), and $KEu(WO_4)_2$ (black).

distances of these compounds are directly observed, showing that both $LiEu(WO_4)_2$ and $NaEu(WO_4)_2$ have the some bond distance distribution and coordination number. The bond-length distribution of $LiEu(WO_4)_2$ is generally shorter than the one of $NaEu(WO_4)_2$, which suggests a lattice contraction phenomenon. For $KEu(WO_4)_2$ with lower crystal symmetry, the W–O bond distance is longer, but the Eu–O bond distance is shorter than the ones of both $LiEu(WO_4)_2$ and $NaEu(WO_4)_2$, which can be understood by bond-valence theory.[22–24] The result of PDF calculation is in good agreement with that of the Rietveld refinement method and gives more precise information about the bond distance distribution and coordination number. Most importantly, it performs more directly than the Rietveld refinement method. The fit was also carried out by the program *PDFgui* (see the Supporting Information, Table S4 and Figures S4–S6). The agreement factor R_{wp} is larger in PDF analysis compared to that in the Rietveld method, which is ascribed to a noise in $G(r)$, the termination ripples, derived from the finite Q_{max} (13.4 Å^{-1}). Good agreement around 30% is also reported.[12,25,26]

Luminescence Properties. Figure 4 presents excitation spectra monitored at 614 nm of $LiEu(WO_4)_2$ and $NaEu(WO_4)_2$ phosphors and at 615 nm of $KEu(WO_4)_2$ phosphor for $^5D_0$–$^7F_2$ emission of Eu^{3+} ions. The excitation spectrum consists of a broad band and some sharp lines. The broad excitation band centered at 270 nm is attributed to the CT transition from oxygen to tungstate and europium. This transition is sensitive to the coordination environment of the Eu^{3+} ions, and the intensity is strongly influenced by the crystal-field environment of the Eu^{3+} ions. In the range from 325 to 550 nm, the characteristic intraconfigurational 4f–4f transition of Eu^{3+} of sharp $^7F_0 \rightarrow {}^5L_6$ transition for 394 nm, $^7F_0 \rightarrow {}^5D_2$ transition for 464 nm, and $^7F_0 \rightarrow {}^5D_1$ transition for 535 nm can be observed.[4] According to the excitation spectrum, it is evident that the $LiEu(WO_4)_2$, $NaEu(WO_4)_2$, and $KEu(WO_4)_2$ phosphors can be excited efficiently by near-ultraviolet (about 396 nm) or blue (about 464 nm) light.[4,10] In Figure 4, the vital difference is only at the 270 nm CT band of oxygen to tungsten (W^{6+}–O^{2-}) and europium (Eu^{3+}–O^{2-}).[27] This process has been known as "host-sensitized" energy transfer. The dotted box shows that the intensity of CT excitation of $KEu(WO_4)_2$ is more effective than that of both $LiEu(WO_4)_2$ and $NaEu(WO_4)_2$. The energy transfer from the absorbing group to the rare-earth ion was ascribed by Dexter to an exchange mechanism.[28] Furthermore, the superexchange between paramagnetic ions depends on the angle in paramagnetic ion–oxygen ion–paramagnetic ion.[29,30] This interaction is usually strong if the angle is 180° (using σ bonding) and considerably weaker for 90° (using π bonding). A similar discussion has been invoked by Van Uitert et al. to explain the concentration quenching of luminescence of Eu^{3+}.[31] For alkali-metal europium double tungstate compounds, the maximum bond angle of W–O–Eu for $LiEu(WO_4)_2$ and $NaEu(WO_4)_2$ is about 143°, while for $KEu(WO_4)_2$, the maximum W–O–Eu angle is about 176°. This means more efficient energy transfer from the host

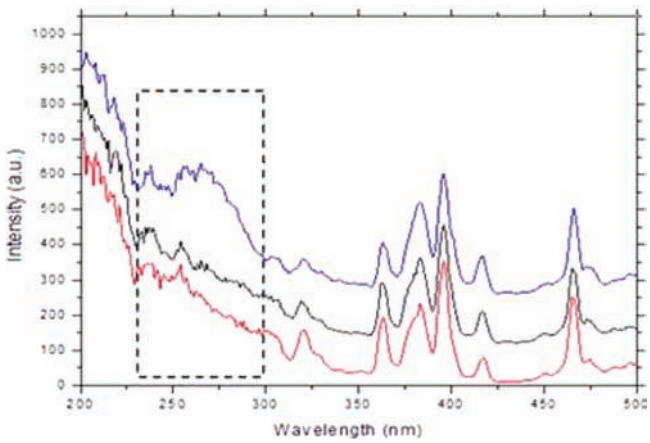

Figure 4. Excitation spectrum for the 615 nm emission of the phosphors $LiEu(WO_4)_2$ (black), $NaEu(WO_4)_2$ (red), and $KEu(WO_4)_2$ (blue) sintered at 750 °C for 10 h. The dotted box represents the CT bands of these compounds.

dx.doi.org/10.1021/ic2013528 | Inorg. Chem. 2011, 50, 11487–11492

matrix to the luminescent center for $KEu(WO_4)_2$ than for both $LiEu(WO_4)_2$ and $NaEu(WO_4)_2$. From Figure 4, the excitation spectra of an intraconfigurational 4f–4f transition remained unchanged for all alkali-metal europium double tungstate compounds because of the well-shielded 4f intershell, avoiding the disturbance from the surroundings (see Table 2 and Figure 3).

Figure 5 shows the emission spectra of $LiEu(WO_4)_2$ and $NaEu(WO_4)_2$ at 396 nm and $KEu(WO_4)_2$ at 395 nm light

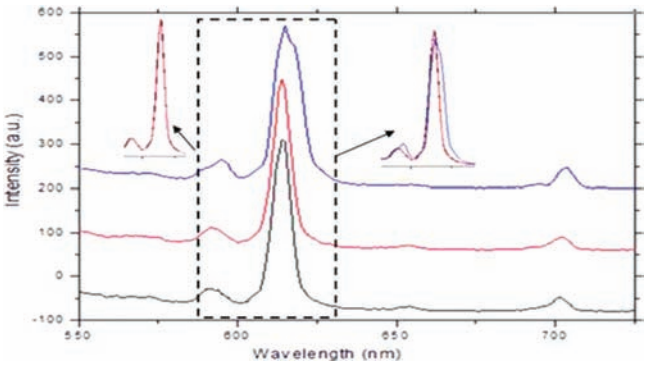

Figure 5. Emission spectra of $LiEu(WO_4)_2$ (black), $NaEu(WO_4)_2$ (red), and $KEu(WO_4)_2$ (blue). Left Inset: difference of $LiEu(WO_4)_2$ and $NaEu(WO_4)_2$. Right inset: difference of $LiEu(WO_4)_2$, $NaEu(WO_4)_2$, and $KEu(WO_4)_2$.

Table 3. $^5D_0$–$^7F_2$ Relative Intensities of $LiEu(WO_4)_2$, $NaEu(WO_4)_2$, and $KEu(WO_4)_2$

phosphor	excitation wavelength (nm)	emission wavelength (nm)	$^5D_0$–$^7F_2$ relative intensity
$LiEu(WO_4)_2$	396	614	1.04
$NaEu(WO_4)_2$	396	614	1.04
$KEu(WO_4)_2$	395	615	1.00[a]

[a]The intensity of $KEu(WO_4)_2$ is regarded as 1.00.

excitation. Table 3 gives a comparison between the emission intensities of $LiEu(WO_4)_2$ and $NaEu(WO_4)_2$ under excitation of 396 nm and of $KEu(WO_4)_2$ at 395 nm. The spectra essentially consists of several sharp lines with wavelengths ranging from 580 to 710 nm, which are associated with the $^5D_0 \rightarrow {}^7F_J$ (J = 1–4) transitions from the excited-state levels of Eu^{3+} to the ground state. The major emissions of $LiEu(WO_4)_2$ and $NaEu(WO_4)_2$ were found at about 614 nm and that of $KEu(WO_4)_2$ was found at 615 nm ($^5D_0 \rightarrow {}^7F_2$), which correspond to red emission of the hypersensitivity transition for trivalent europium. In addition, three weak emission lines at 590 nm ($^5D_0 \rightarrow {}^7F_1$), 654 nm ($^5D_0 \rightarrow {}^7F_3$), and 702 nm ($^5D_0 \rightarrow {}^7F_4$) can also be observed. From Figure 5, the emission spectra of $KEu(WO_4)_2$ appears broader than the ones of both $LiEu(WO_4)_2$ and $NaEu(WO_4)_2$. Blasse[27] pointed out that when excited, the lattice vibration results in a deviation of the metal–ligand distance (R) from that of the ground state (R_0). For $KEu(WO_4)_2$, the presence of K^+ ions with a larger radius affords softer surroundings around the luminescence center, which results in a larger deviation ($\triangle R$), thus producing a larger Stokes shift and a broader optical bands. In addition, the lower crystal symmetry of $KEu(WO_4)_2$ may also contribute to the large Stokes shift and broader optical bands of $KEu(WO_4)_2$. On the other hand, the same Eu–O bond distances of $LiEu(WO_4)_2$ and $NaEu(WO_4)_2$ (see Figures 3 and 5) lead to well-overlapping peaks of the emission spectra.

CONCLUSION

The present study investigates the luminescent properties of $LiEu(WO_4)_2$, $NaEu(WO_4)_2$, and $KEu(WO_4)_2$ by Rietveld and PDF analysis. Both $LiEu(WO_4)_2$ and $NaEu(WO_4)_2$ have the same luminescent properties, in which the identical local surroundings of Eu^{3+} ions are revealed by PDF analysis. For $KEu(WO_4)_2$, the more effective CT excitation, the larger Stokes shift, and the broader optical bands than those of both $LiEu(WO_4)_2$ and $NaEu(WO_4)_2$ are observed, which is in good agreement with the crystal structures discussed. The results obtained by the PDF experimental method are also confirmed by bond-valence theory. The dual-space technique combining Rietveld and PDF analysis offers a powerful tool to revealing correlation of the luminescence properties with the local environment of the emission center through study of the local and average structures of the host matrix.

ASSOCIATED CONTENT

Supporting Information

Rietveld and PDF refinement results. This material is available free of charge via the Internet at http://pubs.acs.org.

AUTHOR INFORMATION

Corresponding Author

*E-mail: hjinping@shnu.edu.cn.

ACKNOWLEDGMENTS

We are grateful to Professor Lv Guanglie at Zhejiang University and Gao Zhongmin at Ji Lin University for providing the beneficial discussion on this paper.

REFERENCES

(1) Moine, B.; Bizarri, G. *Opt. Mater.* **2006**, *28*, 58–63.
(2) Ronda, C. *Luminescence: From Theory to Applications*; Wiley-VCH: Weinheim, Germany, 2007.
(3) Kitai, A. *Luminescent Materials and Applications*; John Wiley & Sons: London, 2008.
(4) Neeraj, S.; Kijima, N.; Cheetham, A. K. *Chem. Phys. Lett.* **2004**, *387*, 2–6.
(5) Van Uitert, L. G.; Soden, R. R. *J. Chem. Phys.* **1962**, *36*, 517.
(6) Shi, S.; Gao, J.; Zhou, J. *Opt. Mater.* **2008**, *30*, 1616–1620.
(7) Li, X.; Yang, Z.; Guan, L.; Guo, J.; Wang, Y.; Guo, Q. *J. Alloys Compd.* **2009**, 684–686.
(8) Liu, J.; Lian, H.; Shi, C. *Opt. Mater.* **2007**, *29*, 1591–1594.
(9) Guo, C.; Wang, S.; Chen, T.; Luan, L.; Xu, Y. *Appl. Phys. A: Mater. Sci. Process.* **2009**, *94*, 365–371.
(10) Shao, Q.; Li, H.; Wu, K.; Dong, Y.; Jiang, J. *J. Lumin.* **2009**, *129*, 879–883.
(11) Chiu, C.; Wang, M.; Lee, C.; Chen, T. *J. Solid State Chem.* **2007**, *180*, 619–627.
(12) Egami, T.; Billinge, S. J. L. *Underneath the Bragg peaks: structural analysis of complex materials*; Pergamon Press Elsevier: Oxford, England, 2003.
(13) Qiu, X.; Thompson, J. W.; Billinge, S. J. L. *J. Appl. Crystallogr.* **2004**, *37*, 678.
(14) Farrow, C. L.; Juhas, P.; Liu, J. W.; Bryndin, D.; Bo, V. Z. I. E. S.; Bloch, J.; Proffen, T.; Billinge, S. J. L. *J. Phys.: Condens. Matter* **2007**, *19*, 335219.
(15) Macalik, L.; Tomaszewski, P. E.; Lisiecki, R.; Hanuza, J. *J. Solid State Chem.* **2008**, 2591–2600.

(16) Gallucci, E.; Goutaudier, C.; Cohen-Adad, M. T.; Mentzen, B. F.; Hansen, T. *J. Alloys Compd.* **2000**, *306*, 227−234.
(17) Larson, A. C.; Von Dreele, R. B. *Los Alamos National Laboratory Report LAUR*; Los Alamos National Laboratory: Los Alamos, NM, 2004; pp 86−748.
(18) Finger, L. W.; Cox, D. E.; Jephcoat, A. P. *J. Appl. Crystallogr.* **1994**, *27*, 892−900.
(19) Huheey, J. E.; Keiter, E. A.; Keiter, R. L. *Inorganic Chemistry: Principles of Structure and Reactivity*, 4th ed.; Harper Collins: New York, 1993.
(20) Winter, M. J. The University of Sheffield and WebElements Ltd., Sheffield, U.K.
(21) Shannon, R. D. *Acta Crystallogr., Sect. A* **1976**, *32*, 751.
(22) Brown, I. D.; Shannon, R. D. *Acta Crystallogr., Sect. A* **1973**, *29*, 266−282.
(23) Brown, I. D.; Wu, K. K. *Acta Crystallogr., Sect. B* **1976**, *32*, 1957−1959.
(24) Murrel, J. N.; Sons, S. F. T. *The Chemical Bond*; John Wiley & Sons: New York, 1985.
(25) Brühne, S.; Gottlieb, S.; Assmus, W.; Alig, E.; Schmidt, M. U. *Cryst. Growth Des.* **2008**, *8*, 489−493.
(26) Page, K.; Hood, T. C.; Proffen, T.; Neder, R. B. *J. Appl. Crystallogr.* **2011**, *44*, 327−336.
(27) Grabmaier, G. B. A. B. *Luminescent Materials*; Springer-Verlag Telos: New York, 1994.
(28) Dexter, D. L. *J. Chem. Phys.* **1953**, *21*, 836−850.
(29) Blasse, G.; Bril, A. *J. Chem. Phys.* **1966**, *45*, 2350−2355.
(30) Gilleo, M. *Phys. Rev.* **1958**, *109*, 777−781.
(31) Van Uitert, L. G.; Linares, R. C.; Soden, R. R.; Ballman, A. A. *J. Chem. Phys.* **1962**, *36*, 702.